

Iron(III) Porphyrin Complexes with Axial Alkyl and Acyl Ligands. Structures and Reactivity of the Acyl Complex toward Dioxygen

Alan L. Balch,* Marilyn M. Olmstead, Nasser Safari, and Tamara N. St. Claire

Department of Chemistry, University of California, Davis, California 95616

Received December 22, 1993^o

Two highly reactive, low-spin ($S = 1/2$) iron(III) porphyrin complexes, one with an axial alkyl ligand and the other with an axial acyl ligand, have been isolated as crystals suitable for single-crystal X-ray diffraction. Red prisms of (TAP)Fe^{III}(CH₃)-THF (TAP is the dianion of tetra-*p*-anisylporphyrin) crystallize in the triclinic space group $P\bar{1}$ with $a = 12.129(2)$ Å, $b = 12.263(3)$ Å, $c = 15.263(2)$ Å, $\alpha = 71.93(2)^\circ$, $\beta = 83.91(2)^\circ$, and $\gamma = 73.92(2)^\circ$ at 130 K with $Z = 2$. Refinement of 586 parameters with 4858 reflections gave $R = 0.069$ and $R_w = 0.076$. The complex consists of a five-coordinate iron which is 0.146 Å out of the N_4 plane with an average Fe–N distance of 1.967 Å and an Fe–C distance of 1.979(9) Å. To accommodate the short Fe–N distances, the porphyrin core is ruffled. Brown plates of (TAP)Fe^{III}(C(O)(*n*-C₄H₉)) crystallize in the monoclinic space group $P2_1/c$ with $a = 16.548(15)$ Å, $b = 18.699(9)$ Å, $c = 15.774(10)$ Å, and $\beta = 118.41(4)^\circ$ at 130 K with $Z = 4$. Refinement of 1774 reflections and 258 parameters yielded $R = 0.060$, $R_w = 0.050$. The iron ion is again five-coordinate with the average Fe–N distance of 1.974 Å and the Fe–C distance of 1.965(12) Å. The iron ion is 0.19 Å out of the N_4 plane. The porphyrin core is ruffled, and the acyl ligand is coordinated in η^1 fashion through carbon. The reaction of several acyl complexes of this type with dioxygen have been examined by ¹H and ²H NMR spectroscopy in order to see whether reactive intermediates form. Oxidation is accompanied by the formation of PFe^{III}OC(O)R and PFe^{III}-OF^{III}P (P is a generic porphyrin dianion). No evidence for the formation of previously characterized ferryl complexes in this process has been found.

Introduction

This article is concerned with two classes of extremely air-sensitive iron(III) porphyrin complexes: those bearing axial alkyl groups and those bearing axial acyl groups. Low-spin ($S = 1/2$), five-coordinate alkyl complexes of the type PFe^{III}R are conveniently prepared by the addition of Grignard reagents or organolithium reagents to the corresponding halide complexes, PFe^{III}Cl.^{1–5} These alkyl complexes readily react with dioxygen in the dark.^{6–9} At –80 °C in toluene solution it is possible to detect the formation of intermediates during the oxygenation process, and these observations indicate that the reaction proceeds by the sequence of reactions shown in eqs 1–3. The first step results in the



conversion for the low-spin alkyl into a high-spin ($S = 5/2$) and highly unstable alkyl peroxide complex. The detection of these alkyl peroxo complexes is particularly significant because of the numerous postulates of the existence of such species in biological processes (peroxidase and catalase activity,¹⁰ lipoxygenation,¹¹ and aromatase reactivity¹²). Even at –80 °C the peroxo species reacts further. When a hydrogen atom is present on the α carbon, the process shown in eq 2 occurs to produce the hydroxo iron porphyrin and an aldehyde or ketone.^{7,8} No other iron porphyrin complex can be detected as an intermediate during this process. However, when no hydrogen atom is present on the α carbon atom of the alkyl peroxide ligand, the peroxide complex undergoes homolytic cleavage of the O–O bond to form a ferryl, (Fe^{IV}O)²⁺, complex and an alkoxy radical as shown in eq 4.



The iron(III) alkyl complexes also react with other small molecules generally to give products of apparent insertions into the iron–carbon bond. Thus with sulfur dioxide, complexes of the type PFe^{III}SO₂R are readily formed.¹³ These are sufficiently stable so that they have been crystallized and studied by X-ray diffraction. In the presence of dioxygen these sulfonato complexes are oxidized to form sulfonato complexes, PFe^{III}SO₃R.¹³ Treatment of PFe^{III}R with carbon monoxide leads to the formation of acyl complexes which have been studied by spectroscopic techniques in solution but not previously isolated.¹⁴ Carbon dioxide is also reported to insert into the Fe–C bond of the alkyl complexes.¹⁴ However, with nitric oxide diamagnetic adducts,

* Abstract published in *Advance ACS Abstracts*, May 15, 1994.

(1) Abbreviations used: P, generic porphyrin dianion; P[•], generic porphyrin radical monoanion; TAP, dianion of tetra-*p*-anisylporphyrin; TMP, dianion of tetramesitylporphyrin; TPP, dianion of tetraphenylporphyrin; R, alkyl group; Ar, aryl group; THF, tetrahydrofuran.

(2) Lexa, D.; Mispelter, J.; Savéant, J.-M. *J. Am. Chem. Soc.* **1981**, *103*, 6806.

(3) Cocolios, P.; Lagrange, G.; Guillard, R. *J. Organomet. Chem.* **1983**, *253*, 65.

(4) Tabard, A.; Cocolios, P.; LaGrange, G.; Gerardin, R.; Hubsch, J.; Lecomte, C.; Zarembowitch, J.; Guillard, R. *Inorg. Chem.* **1988**, *27*, 110.

(5) Gueutin, C.; Lexa, D.; Savéant, J.-M.; Wang, D.-L. *Organometallics* **1989**, *8*, 1607.

(6) Balch, A. L.; Hart, R. L.; Latos-Grażyński, L.; Traylor, T. G. *J. Am. Chem. Soc.* **1990**, *112*, 7382.

(7) Arasasingham, R. D.; Balch, A. L.; Latos-Grażyński, L. *J. Am. Chem. Soc.* **1987**, *109*, 5846.

(8) Arasasingham, R. D.; Balch, A. L.; Cornman, C. R.; Latos-Grażyński, L. *J. Am. Chem. Soc.* **1989**, *111*, 4357.

(9) Balch, A. L.; Cornman, C. R.; Safari, N.; Latos-Grażyński, L. *Organometallics* **1990**, *9*, 2420.

(10) Everse, J.; Everse, K. E.; Grisham, M. B., Eds. *Peroxidases in Chemistry and Biology*; CRC Press: Boca Raton, FL, 1991; Vols. 1 and 2.

(11) Corey, E. J.; Nagata, R. *J. Am. Chem. Soc.* **1987**, *109*, 8107. Corey, E. J.; Walker, J. C. *J. Am. Chem. Soc.* **1987**, *109*, 8108.

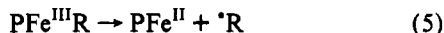
(12) Stevenson, D. E.; Wright, J. N.; Akhtar, M. *J. Chem. Soc., Chem. Commun.* **1985**, 1078. Cole, P. A.; Robinson, C. H. *J. Am. Chem. Soc.* **1988**, *110*, 1284.

(13) Cocolios, P.; Laviron, E.; Guillard, R. *J. Organomet. Chem.* **1982**, *228*, C39. Cocolios, P.; Lagrange, G.; Oumous, H.; Lecomte, C. *J. Chem. Soc., Dalton Trans.* **1984**, 567.

(14) Arafa, I. M.; Shin, K.; Goff, H. M. *J. Am. Chem. Soc.* **1988**, *110*, 5228.

$\text{PFe}(\text{R})(\text{NO})$, are formed which are reported to have the nitric oxide bound *trans* to the alkyl ligand.¹⁵

In addition to their sensitivity toward reaction with small molecules, these iron alkyl complexes are prone to fragmentation to form alkyl radicals via eq 5.⁸ All are light sensitive and need



to be purified and manipulated under low intensity lighting. Additionally the benzyl examples and those with tertiary alkyl groups undergo dissociation via eq 5 at room temperature.⁶

The corresponding iron aryl complexes, $\text{PFe}^{\text{III}}\text{Ar}$, are more stable than their alkyl counterparts.^{4,12-14} (TPP) $\text{Fe}^{\text{III}}\text{Ph}$ has been isolated, crystallized, and examined by X-ray crystallography.¹⁹ This complex shows a typical low-spin structure with the iron only 0.17 Å out of the plane of the four pyrrole nitrogen atoms, an average Fe–N bond length of 1.961 Å, and an Fe–C distance of 1.955(3) Å. These aryl complexes are considerably less reactive toward dioxygen than their alkyl counterparts. In toluene solution phenoxide complexes are formed without the intervention of any detectable intermediate, while in chloroform solution a mixture of the Fe^{IV} aryl complex, $[\text{PFe}^{\text{IV}}\text{Ar}]^+$, and the Fe^{III} chloro complex, $\text{PFe}^{\text{III}}\text{Cl}$, is formed.²⁰

Here we report the results of our efforts to obtain crystalline samples of the alkyl and acyl iron(III) porphyrin complexes that were suitable for X-ray crystallography and would in the case of the acyl distinguish between unidentate and bidentate coordination.²¹ This work was undertaken with the additional goal of examining the reactivity of the acyl complexes with dioxygen. In that case there was an opportunity to prepare an acyl peroxy complex, $\text{PFe}^{\text{III}}(\text{OOC}(\text{O})\text{R})$, if the reaction of $\text{PFe}^{\text{III}}(\text{C}(\text{O})\text{R})$ with dioxygen followed a course analogous to eq 1. Such acyl peroxy complexes are believed to be important precursors to the formation of green ferryl complexes of the type $[(\text{P}^*)\text{Fe}^{\text{IV}}=\text{O}]^+$.²²⁻²⁵ These ferryl complexes, which may be directly detected spectroscopically,^{22,23} are at the same oxidation level as compound I of horseradish peroxidase and are reactive oxidants. Direct observations of (acyl peroxy)iron porphyrin complexes have been described.²⁶⁻²⁹ For example, the reaction of (TMP) $\text{Fe}^{\text{III}}\text{OH}$ with *p*-nitroperoxybenzoic acid forms (TMP)- $\text{Fe}(\text{OOC}(\text{O})\text{C}_6\text{H}_4\text{-}p\text{-NO}_2)$, which reacts further even at -46°C to yield green $[(\text{TMP}^*)\text{Fe}^{\text{IV}}=\text{O}]^+$.²⁶

Results

The iron alkyl complexes, $\text{PFe}^{\text{III}}\text{R}$, were prepared as described previously from $\text{PFe}^{\text{III}}\text{Cl}$ and a Grignard reagent.^{3,8} After chromatography on alumina under a dinitrogen atmosphere and subdued lighting, crystals of (TaP) $\text{Fe}^{\text{III}}(\text{CH}_3)$ were obtained by

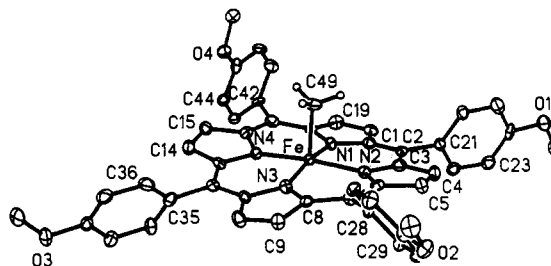


Figure 1. Perspective view of (TAP) $\text{Fe}^{\text{III}}(\text{CH}_3)$ with 50% thermal contours for all atoms.

diffusion of hexane into a solution of the complex in a toluene/THF mixture. The acyl complexes were obtained by addition of carbon monoxide to the alkyl complexes. (TAP) $\text{Fe}^{\text{III}}(\text{C}(\text{O})(n\text{-Bu}))$ was sufficiently stable so that it could be purified by column chromatography on activated alumina with dichloromethane as the eluent. Crystals of this complex were grown by diffusion of hexane into a toluene solution of the complex. This acyl complex is considerably less light sensitive than the corresponding alkyl complex, and its manipulation did not require low lighting conditions. Exposure of a toluene solution of (TAP) $\text{Fe}^{\text{III}}(\text{C}(\text{O})(n\text{-Bu}))$ to white light from a standard slide projector lamp for 7 h did not result in significant loss of the complex, and neither (TAP) Fe^{II} nor (TAP) $\text{Fe}^{\text{III}}(n\text{-Bu})$ was observed to form. Additionally, evaporation of solutions of (TAP) $\text{Fe}^{\text{III}}(\text{C}(\text{O})\text{R})$ can be effected without loss of carbon monoxide.

Structure of (TAP) $\text{Fe}^{\text{III}}(\text{CH}_3)\cdot\text{THF}$. The structure of the complex has been determined by X-ray diffraction. A view of the molecule is given in Figure 1. Atomic positional parameters are presented in Table 1. Table 2 contains selected bond distances and angles.

The complex contains no crystallographically imposed element of symmetry. The iron is five-coordinate with square pyramidal geometry. The structural parameters for the iron are entirely consistent with expectations for low-spin iron(III).³⁰ Thus the iron ion is only 0.146 Å out of the N_4 plane and the average Fe–N distance is 1.967 Å. The Fe–C distance is 1.979(9) Å, which is somewhat longer than that in the low-spin Fe^{III} phenyl complexes, (TPP) $\text{Fe}^{\text{III}}\text{Ph}$ (1.955(3) Å)¹⁹ and $(\text{C}_{22}\text{H}_{22}\text{N}_4)\text{Fe}^{\text{III}}\text{Ph}$ (1.933(3) Å).³¹

The porphyrin core in (TAP) $\text{Fe}^{\text{III}}(\text{CH}_3)$ is strongly ruffled.³² This can be best appreciated by turning to Figure 2, which shows the out-of-plane displacements of the atoms of the core of the porphyrin. This ruffling is probably a result of the shortness of the Fe–N bonds which necessitates some degree of compression of the porphyrin core diameter. Similar ruffling is seen in (TPP)- $\text{Fe}^{\text{III}}\text{Ph}$.¹⁹

The meso anisyl groups display a variety of twists in their orientation relative to the porphyrin plane. The anisyl ring containing C(22) is nearly perpendicular to that plane (dihedral angle, 78.2°). The rings containing C(35), C(42), and C(29) have larger twists with dihedral angles of 62.1° , 56.3° , and 54.1° , respectively. Dihedral angles that are less than 60° are uncommon for porphyrins with a ruffled core geometry.³² Since the iron is present as an electron-deficient, 15-electron center, we wondered whether this twisting might result from some form of additional weak coordination or association in the solid state. Additionally there is the possibility that the THF molecule might interact with the electron-deficient iron center. Consequently the packing of the molecules in the solid was carefully examined.

Figure 3 shows the relationships between three adjacent molecules of the complex and the three adjoining THF molecules. The THF molecules are disordered and only one of the two equally populated orientations is shown in this drawing. Nevertheless it

- (15) Guilard, R.; Lagrange, G.; Tabard, A.; Lancon, D.; Kadish, K. M. *Inorg. Chem.* **1985**, *24*, 3649.
- (16) Ogoshi, H.; Sugimoto, H.; Yoshida, Z.-I.; Kobayashi, H.; Sakai, H.; Maeda, Y. *J. Organomet. Chem.* **1982**, *234*, 185.
- (17) Ortiz de Montellano, P. R.; Kunze, K. L. *J. Am. Chem. Soc.* **1981**, *103*, 6534.
- (18) Balch, A. L.; Renner, M. W. *Inorg. Chem.* **1986**, *25*, 303.
- (19) Doppelt, P. *Inorg. Chem.* **1984**, *23*, 4009.
- (20) Arasasingham, R. D.; Balch, A. L.; Hart, R. L.; Latos-Grażyński, L. *J. Am. Chem. Soc.* **1990**, *112*, 7566.
- (21) Hermes, A. R.; Girolami, G. S. *Organometallics* **1988**, *7*, 394.
- (22) Groves, J. T.; Haushalter, R. C.; Nakamura, M.; Nemo, T. E.; Evans, B. J. *J. Am. Chem. Soc.* **1981**, *103*, 2884.
- (23) Balch, A. L.; Latos-Grażyński, L.; Renner, M. W. *J. Am. Chem. Soc.* **1985**, *107*, 2983.
- (24) Traylor, T. G.; Lee, W. A.; Stynes, D. V. *J. Am. Chem. Soc.* **1984**, *106*, 755.
- (25) Lee, W. A.; Bruce, T. C. *J. Am. Chem. Soc.* **1985**, *107*, 513. Balasubramanian, P. N.; Lee, R. W.; Bruce, T. C. *J. Am. Chem. Soc.* **1989**, *111*, 8714. Ostovic, D.; Bruce, T. C. *Acc. Chem. Res.* **1992**, *25*, 314.
- (26) Groves, J. T.; Watanabe, Y. *J. Am. Chem. Soc.* **1986**, *108*, 7834.
- (27) Groves, J. T.; Watanabe, Y. *J. Am. Chem. Soc.* **1986**, *108*, 7836.
- (28) Groves, J. T.; Watanabe, Y. *Inorg. Chem.* **1987**, *26*, 785.
- (29) Yamaguchi, K.; Watanabe, Y.; Morishima, I. *J. Am. Chem. Soc.* **1993**, *115*, 4058.

(30) Scheidt, W. R.; Reed, C. A. *Chem. Rev.* **1981**, *81*, 543.

(31) Goedken, V. L.; Peng, S.-M.; Park, Y. *J. Am. Chem. Soc.* **1974**, *96*, 284.

(32) Scheidt, W. R.; Lee, Y. *J. Struct. Bonding* **1987**, *64*, 1.

Table 1. Atomic Coordinates ($\times 10^4$) and Equivalent Isotropic Displacement Coefficients ($\text{\AA}^2 \times 10^3$) for $(\text{TAP})\text{Fe}^{\text{III}}(\text{CH}_3)\cdot\text{THF}$

| | <i>x</i> | <i>y</i> | <i>z</i> | <i>U</i> (eq) ^a |
|--------|----------|----------|----------|----------------------------|
| Fe | 3652(1) | 2906(1) | 648(1) | 12(1) |
| O(1) | 7716(4) | 4304(4) | -4736(3) | 30(2) |
| O(2) | 8962(4) | -3981(4) | 3096(3) | 23(2) |
| O(3) | -1295(4) | 1321(4) | 5493(3) | 29(2) |
| O(4) | -813(4) | 10422(4) | -1362(3) | 24(2) |
| N(1) | 3436(4) | 4157(4) | -544(3) | 15(2) |
| N(2) | 4997(4) | 1961(4) | 127(3) | 15(2) |
| N(3) | 3692(4) | 1533(4) | 1741(3) | 17(2) |
| N(4) | 2204(4) | 3769(4) | 1104(3) | 16(2) |
| C(1) | 4093(5) | 4183(5) | -1345(4) | 18(2) |
| C(2) | 5102(5) | 3335(5) | -1428(4) | 15(2) |
| C(3) | 5504(5) | 2291(5) | -731(4) | 19(2) |
| C(4) | 6561(5) | 1428(5) | -816(4) | 21(2) |
| C(5) | 6710(5) | 563(6) | 0(4) | 21(2) |
| C(6) | 5743(5) | 882(5) | 580(4) | 16(2) |
| C(7) | 5544(5) | 201(5) | 1471(4) | 17(2) |
| C(8) | 4547(5) | 472(5) | 1986(4) | 16(2) |
| C(9) | 4250(5) | -313(5) | 2811(4) | 20(2) |
| C(10) | 3212(5) | 249(5) | 3104(5) | 24(2) |
| C(11) | 2884(5) | 1388(5) | 2448(4) | 16(2) |
| C(12) | 1903(5) | 2267(5) | 2556(4) | 15(2) |
| C(13) | 1634(5) | 3397(5) | 1941(4) | 17(2) |
| C(14) | 730(5) | 4357(6) | 2093(4) | 22(2) |
| C(15) | 749(5) | 5318(5) | 1374(4) | 21(2) |
| C(16) | 1633(5) | 4960(5) | 746(4) | 17(2) |
| C(17) | 1813(5) | 5669(5) | -129(4) | 20(2) |
| C(18) | 2622(5) | 5243(5) | -749(4) | 16(2) |
| C(19) | 2734(5) | 5897(5) | -1693(4) | 21(2) |
| C(20) | 3645(5) | 5246(5) | -2055(4) | 20(2) |
| C(21) | 5775(5) | 3575(5) | -2315(4) | 18(2) |
| C(22) | 5408(6) | 3479(5) | -3101(4) | 22(2) |
| C(23) | 6036(6) | 3706(6) | -3936(4) | 23(2) |
| C(24) | 7045(5) | 4032(6) | -3953(4) | 23(2) |
| C(25) | 7422(6) | 4152(6) | -3171(5) | 29(3) |
| C(26) | 6798(5) | 3901(6) | -2351(4) | 20(2) |
| C(27) | 7307(7) | 4249(7) | -5566(5) | 32(3) |
| C(28) | 6445(5) | -899(5) | 1896(4) | 17(2) |
| C(29) | 6852(5) | -1822(5) | 1502(4) | 17(2) |
| C(30) | 7695(5) | -2834(5) | 1908(4) | 20(2) |
| C(31) | 8129(5) | -2951(5) | 2747(4) | 19(2) |
| C(32) | 7729(5) | -2059(6) | 3170(4) | 23(2) |
| C(33) | 6902(5) | -1043(5) | 2740(4) | 18(2) |
| C(34) | 9426(6) | -4139(6) | 3962(4) | 28(2) |
| C(35) | 1100(5) | 1970(5) | 3348(4) | 19(2) |
| C(36) | 1410(6) | 1732(6) | 4262(5) | 25(2) |
| C(37) | 641(6) | 1500(6) | 4995(5) | 27(2) |
| C(38) | -467(6) | 1518(5) | 4825(4) | 22(2) |
| C(39) | -780(5) | 1715(6) | 3921(4) | 22(2) |
| C(40) | -13(5) | 1959(5) | 3203(4) | 21(2) |
| C(41) | -1021(6) | 1260(6) | 6407(4) | 28(2) |
| C(42) | 1119(5) | 6923(5) | -445(4) | 15(2) |
| C(43) | -70(5) | 7212(5) | -527(4) | 18(2) |
| C(44) | -691(5) | 8393(5) | -821(4) | 20(2) |
| C(45) | -119(5) | 9288(6) | -1064(4) | 21(2) |
| C(46) | 1060(5) | 9016(5) | -1000(5) | 23(2) |
| C(47) | 1673(5) | 7835(6) | -683(5) | 23(2) |
| C(48) | -282(6) | 11377(5) | -1503(5) | 26(2) |
| C(49) | 4646(6) | 3630(6) | 1116(5) | 30(3) |
| O(5A) | 5161(26) | 2049(21) | 5059(14) | 130(14) |
| O(5B) | 4242(14) | 1553(14) | 5013(9) | 69(6) |
| C(50A) | 5960(20) | 1495(42) | 4493(31) | 109(21) |
| C(50B) | 5417(30) | 1217(34) | 4572(19) | 122(17) |
| C(51) | 5389(12) | 1920(9) | 3628(9) | 87(6) |
| C(52) | 4373(10) | 2963(10) | 3653(7) | 75(5) |
| C(53) | 4020(10) | 2754(10) | 4646(8) | 66(5) |

^a Equivalent isotropic *U* defined as one-third of the trace of the orthogonalized U_{ij} tensor. Disordered atoms of THF refined with 0.5 occupancy.

is apparent that the THF molecules are not near the vacant coordination site on the iron. Indeed the closest approach of any ring atom of THF to iron is 4.78 Å and that approach is on the same face as the axial methyl group. As Figure 3 shows, the closest approach between one iron and the adjacent porphyrin on the exposed face involves H(29) of one of the anisyl rings. The

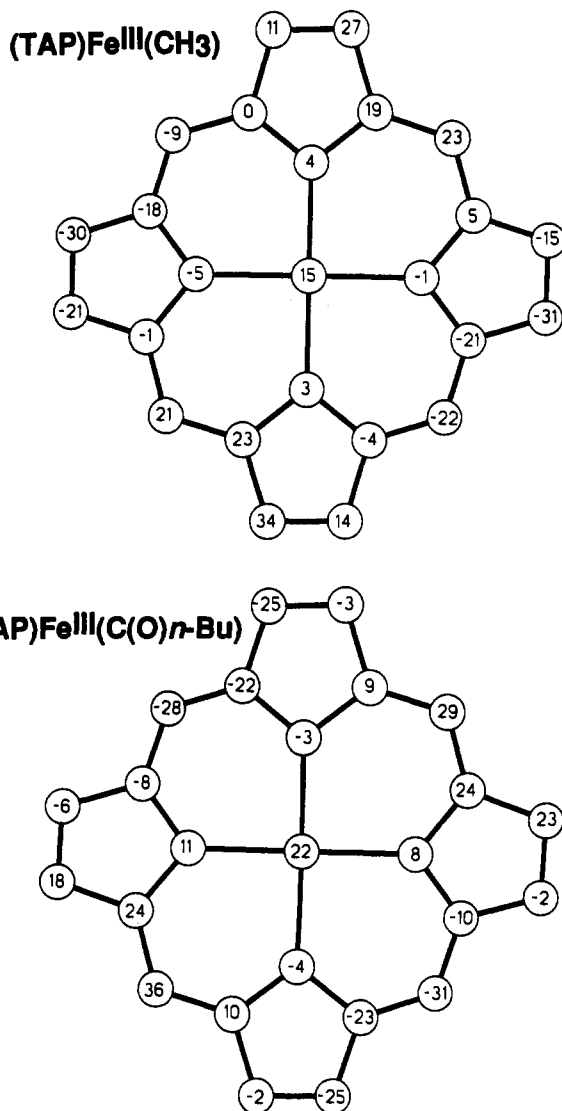


Figure 2. Diagram of the porphyrin cores of A, $(\text{TAP})\text{Fe}^{\text{III}}(\text{CH}_3)$, and B, $(\text{TAP})\text{Fe}^{\text{III}}(\text{C}(\text{O})(n\text{-Bu}))$, in which each atom symbol is replaced by a number that shows the displacement (in 0.01 Å) of that atom from the mean plane of the iron, the 4 nitrogen atoms, and the 20 carbon atoms of the porphyrin core.

Table 2. Selected Bond Lengths and Angles for $(\text{TAP})\text{Fe}^{\text{III}}(\text{CH}_3)\cdot\text{THF}$

| Bond lengths (Å) | | | |
|-------------------|----------|---------------|----------|
| Fe-N(1) | 1.970(4) | Fe-N(2) | 1.971(5) |
| Fe-N(3) | 1.961(5) | Fe-N(4) | 1.964(5) |
| Fe-C(49) | 1.979(9) | | |
| Bond Angles (deg) | | | |
| N(1)-Fe-N(2) | 90.0(2) | N(1)-Fe-N(3) | 169.5(3) |
| N(2)-Fe-N(3) | 89.6(2) | N(1)-Fe-N(4) | 89.3(2) |
| N(2)-Fe-N(4) | 173.4(3) | N(3)-Fe-N(4) | 89.9(2) |
| N(1)-Fe-C(49) | 93.2(3) | N(2)-Fe-C(49) | 91.0(3) |
| N(3)-Fe-C(49) | 97.3(3) | N(4)-Fe-C(49) | 95.5(3) |

Fe...H(29) distance is 3.20 Å, which is too long to represent any sort of significant chemical bonding. Since the porphyrins are arranged so that anisyl groups of one porphyrin overlap with the flat porphyrin core of another molecule, twisting of the anisyl group appears to result from packing effects. Additionally, it is apparent that the anisyl oxygen atoms do not interact with the iron ions of adjacent porphyrins.

Structure of $(\text{TAP})\text{Fe}^{\text{III}}(\text{C}(\text{O})(n\text{-Bu}))$. The geometry of this compound has been determined by single-crystal X-ray diffraction. A drawing of the molecule is given in Figure 4. Table 3 contains atomic positional parameters, while Table 4 contains selected bond distances and angles.

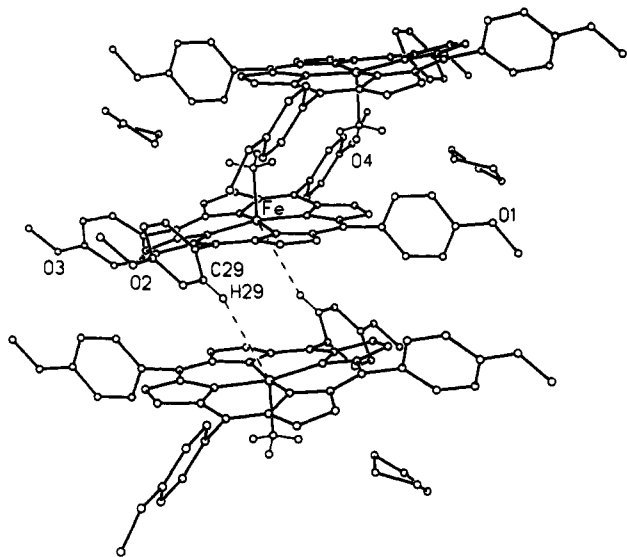


Figure 3. Diagram that shows the relative orientations of three molecules of (TAP)Fe^{III}(CH₃) and three THF molecules in the solid state. Only one of the two THF orientations is shown.

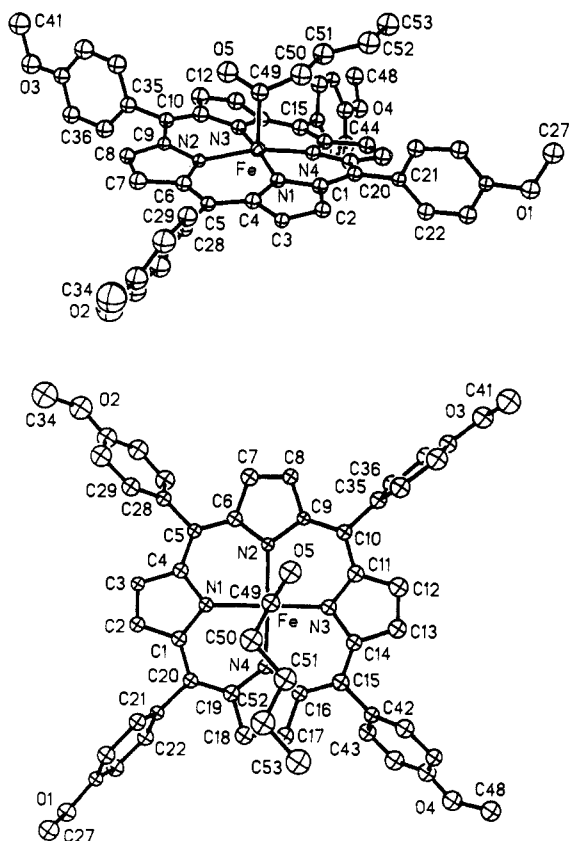


Figure 4. Two views of (TAP)Fe^{III}(C(O)(*n*-Bu)) with 50% thermal contours for all atoms.

The complex contains a five-coordinate iron with a structure that is similar in major components to that of (TAP)Fe^{III}(CH₃) and TPPFe^{III}Ph. Thus the geometric parameters for the iron atom are consistent with the presence of low-spin Fe^{III}. The average Fe–N distance is 1.974 Å, and the Fe–N₄ plane distance is 0.19 Å. The Fe–C distance is 1.965(12) Å, which is within the experimental error the same as that in the methyl complex.

The acyl group in this electron-deficient, 15-electron complex is clearly monodentate with an Fe...O separation (2.752(9) Å) that is much longer than the Fe–C bond distance and in the range reported for monodentate acyl groups.²¹ The other distances within the acyl group are normal. The C(5)–O(49) distance is 1.204(19) Å, and the *n*-butyl chain adopts a zigzag planar

Table 3. Atomic Coordinates ($\times 10^4$) and Equivalent Isotropic Displacement Coefficients ($\text{\AA}^2 \times 10^3$) for (TAP)Fe^{III}(C(O)(*n*-Bu))

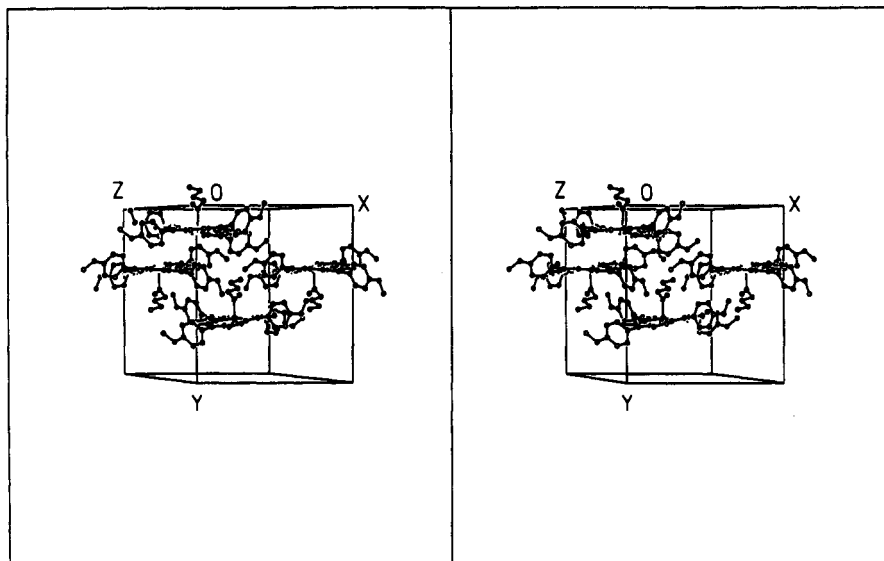
| | <i>x</i> | <i>y</i> | <i>z</i> | <i>U</i> (eq) ^a |
|-------|-----------|----------|----------|----------------------------|
| Fe | 8141(1) | 3683(1) | 1095(1) | 22(1) |
| N(1) | 9280(6) | 3541(5) | 1000(7) | 21(3) |
| N(2) | 8855(6) | 3504(5) | 2506(6) | 17(3) |
| N(3) | 6989(6) | 3688(6) | 1172(7) | 24(3) |
| N(4) | 7433(7) | 3584(5) | -309(7) | 23(3) |
| O(1) | 9397(5) | 4192(4) | -3844(6) | 33(2) |
| O(2) | 14046(6) | 2537(5) | 5387(6) | 58(3) |
| O(3) | 6469(6) | 4054(5) | 5760(6) | 45(3) |
| O(4) | 2087(6) | 3094(5) | -3240(6) | 44(3) |
| O(5) | 8255(6) | 5003(5) | 1915(6) | 45(3) |
| C(1) | 9374(8) | 3599(7) | 179(8) | 24(3) |
| C(2) | 10320(8) | 3498(6) | 426(8) | 24(4) |
| C(3) | 10786(8) | 3343(6) | 1354(8) | 19(3) |
| C(4) | 10159(8) | 3380(6) | 1741(9) | 24(4) |
| C(5) | 10387(8) | 3260(6) | 2695(8) | 20(3) |
| C(6) | 9774(8) | 3340(6) | 3042(9) | 25(4) |
| C(7) | 10004(9) | 3314(6) | 4036(9) | 30(4) |
| C(8) | 9257(8) | 3486(6) | 4108(9) | 24(4) |
| C(9) | 8520(8) | 3597(6) | 3170(8) | 17(3) |
| C(10) | 7621(8) | 3765(7) | 2926(8) | 24(3) |
| C(11) | 6906(8) | 3786(7) | 3786(7) | 29(4) |
| C(12) | 5964(8) | 3848(7) | 1772(9) | 38(4) |
| C(13) | 5460(8) | 3743(7) | 808(8) | 35(4) |
| C(14) | 6082(8) | 3653(7) | 405(8) | 25(3) |
| C(15) | 5836(8) | 3551(7) | -546(9) | 30(4) |
| C(16) | 6467(8) | 3546(7) | -883(9) | 24(4) |
| C(17) | 6228(9) | 3552(7) | -1891(9) | 30(4) |
| C(18) | 7009(8) | 3615(7) | -1935(9) | 34(4) |
| C(19) | 7754(9) | 3632(7) | -982(9) | 28(4) |
| C(20) | 8670(8) | 3707(7) | -748(8) | 22(3) |
| C(21) | 8912(8) | 3825(7) | -1533(8) | 20(3) |
| C(22) | 8801(8) | 3302(7) | -2207(8) | 28(4) |
| C(23) | 8997(8) | 3438(7) | -2937(9) | 30(4) |
| C(24) | 9263(8) | 4121(7) | -3063(8) | 20(3) |
| C(25) | 9377(8) | 4648(7) | -2401(8) | 29(4) |
| C(26) | 9200(8) | 4492(7) | -1653(9) | 27(4) |
| C(27) | 9538(8) | 4905(6) | -4070(8) | 38(4) |
| C(28) | 11354(8) | 3097(7) | 3391(8) | 24(3) |
| C(29) | 12060(8) | 3552(7) | 3564(8) | 33(4) |
| C(30) | 12978(9) | 3396(7) | 4215(9) | 45(4) |
| C(31) | 13156(10) | 2765(8) | 4713(10) | 42(4) |
| C(32) | 12474(9) | 2289(7) | 4548(9) | 44(4) |
| C(33) | 11574(9) | 2434(7) | 3869(9) | 41(4) |
| C(34) | 14784(9) | 3019(7) | 5545(10) | 69(5) |
| C(35) | 7385(8) | 3858(7) | 3716(9) | 28(4) |
| C(36) | 7232(8) | 3280(7) | 4155(9) | 35(4) |
| C(37) | 6951(8) | 3354(7) | 4859(9) | 34(4) |
| C(38) | 6792(9) | 4019(7) | 5106(9) | 30(4) |
| C(39) | 6912(8) | 4620(8) | 4665(9) | 43(4) |
| C(40) | 7230(8) | 4531(7) | 3989(9) | 39(4) |
| C(41) | 6318(9) | 4747(7) | 6040(9) | 56(5) |
| C(42) | 4829(8) | 3467(6) | -1267(8) | 25(4) |
| C(43) | 4539(8) | 2824(7) | -1788(8) | 34(4) |
| C(44) | 3614(9) | 2729(7) | -2439(9) | 42(4) |
| C(45) | 2993(9) | 3254(7) | -2567(9) | 36(4) |
| C(46) | 3251(8) | 3896(6) | -2076(8) | 28(4) |
| C(47) | 4182(8) | 3998(7) | -1446(8) | 34(4) |
| C(48) | 1384(8) | 3570(6) | -3309(8) | 43(4) |
| C(49) | 8221(9) | 4730(6) | 1207(10) | 30(3) |
| C(50) | 8183(8) | 5154(8) | 399(9) | 45(4) |
| C(51) | 7188(8) | 5332(7) | -362(9) | 45(4) |
| C(52) | 7131(8) | 5650(7) | -1284(9) | 50(5) |
| C(53) | 6137(8) | 5807(7) | -2018(9) | 53(4) |

^a Equivalent isotropic *U* defined as one-third of the trace of the orthogonalized *U*_{*ij*} tensor.

conformation. The acyl group is tilted with respect to the frame of the Fe–N axes. The O(5)–C(49)–Fe–N(2) dihedral angle is 31.1°.

As with (TAP)Fe^{III}(CH₃), the porphyrin in (TAP)Fe^{III}(C(O)(*n*-Bu)) displays a significant ruffling. This is readily apparent in the formal diagram in Figure 2 which compares the core displacements of the two complexes.

The phenyl groups in (TAP)Fe^{III}(C(O)(*n*-Bu)) show unusual orientations. The two that involve C(35)–C(40) and C(21)–C(26) are nearly perpendicular to the porphyrin plane with

Figure 5. Packing diagram for (TAP)Fe^{III}(C(O)(*n*-Bu)).Table 4. Selected Bond Lengths and Angles for (TAP)Fe^{III}(C(O)(*n*-Bu))

| Bond Lengths (Å) | | | |
|------------------|-----------|-------------|-----------|
| Fe-N(1) | 1.978(12) | Fe-N(2) | 1.990(9) |
| Fe-N(3) | 1.968(12) | Fe-N(4) | 1.961(10) |
| Fe-C(49) | 1.965(12) | O(5)-C(49) | 1.204(19) |
| C(50)-C(51) | 1.544(15) | C(49)-C(50) | 1.477(22) |
| C(52)-C(53) | 1.524(15) | C(51)-C(52) | 1.532(21) |

| Bond Angles (deg) | | | |
|-------------------|-----------|----------------------|-----------|
| N(1)-Fe-N(2) | 89.0(4) | N(1)-Fe-N(3) | 172.5(4) |
| N(2)-Fe-N(3) | 90.5(4) | N(1)-Fe-N(4) | 88.9(5) |
| N(2)-Fe-N(4) | 164.9(4) | N(3)-Fe-N(4) | 89.7(5) |
| N(1)-Fe-C(49) | 96.6(6) | N(2)-Fe-C(49) | 95.1(5) |
| N(3)-Fe-C(49) | 90.8(6) | N(4)-Fe-C(49) | 100.0(5) |
| Fe-C(49)-O(5) | 118.5(11) | Fe-C(49)-C(50)-C(51) | 112.2(13) |
| O(5)-C(49)-C(50) | 122.5(11) | C(49)-C(50)-C(51) | 112.2(13) |
| C(50)-C(51)-C(52) | 112.5(13) | C(51)-C(52)-C(53) | 110.6(12) |

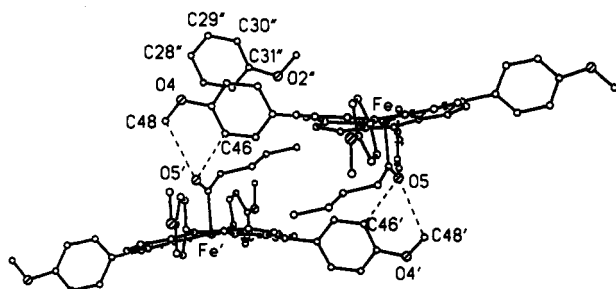
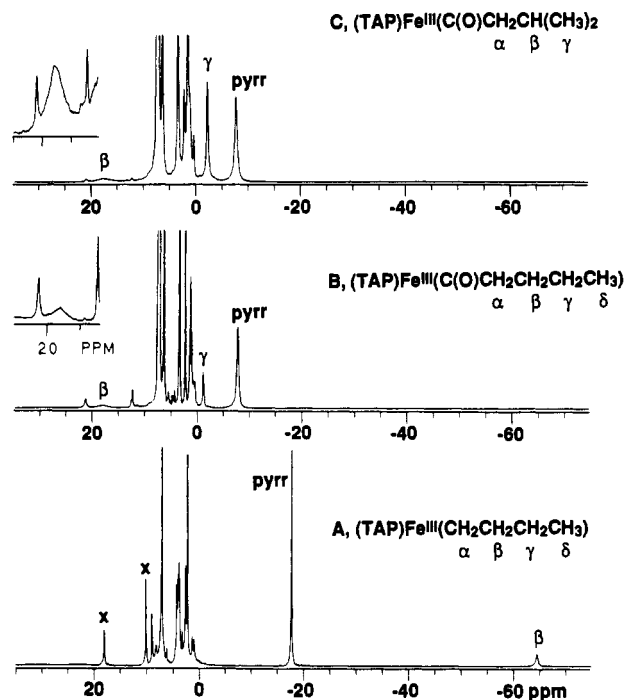


Figure 6. Diagram that shows the relationships between the anisyl group of one porphyrin with the acyl group on another molecule and the face to face orientation of that anisyl group with a different anisyl group on a third molecule.

dihedral angles of 87.6 and 79.1°. The other two rings (involving C(28)-C(33) and C(42)-C(47)) are markedly twisted from the perpendicular arrangement with dihedral angles of 65.8 and 66.3°. This asymmetry is related to the molecular packing in the solid state as Figures 5 and 6 show. The anisyl group C(42)-C(47)-O(4)-C(48) interacts with the carbonyl group on an adjacent molecule as shown in Figure 6. The C(46)-C(45)-O-C(40) unit effectively forms a chelating unit about that carbonyl group with distances C(46)···O(5) = 3.33 Å and C(40)···O(5) = 3.32 Å. These contacts appear to reflect the presence of C-H···O hydrogen bonds.³³ The orientation of this anisyl group in turn effects the orientation of the phenyl group consisting of C(26)-C(31) on an adjacent molecule. These two rings are stacked in face-to-face

(33) Taylor, R.; Kennard, O. *J. Am. Chem. Soc.* **1982**, *104*, 5063. Desiraju, G. R. *Acc. Chem. Res.* **1991**, *24*, 290.

Figure 7. 300-MHz ¹H NMR spectra of toluene-*d*₈ solutions of A, (TAP)Fe^{III}(*n*-Bu), B, (TAP)Fe^{III}(C(O)(*n*-Bu)), and C, (TAP)Fe^{III}(C(O)(*i*-Bu)) at 25 °C. Resonance assignments are given by pyrr, pyrrole protons and β and γ, and β and γ protons of the axial alkyl ligands. Resonances of (TAP)Fe^{II} are labeled X.

fashion. As a result the two anisyl groups at opposite ends of (TAP)Fe^{III}(C(O)(*n*-Bu)) are twisted so that they do not lie perpendicular to the porphyrin core.

Reactivity of Acyl Iron Complexes with Dioxygen. The reactivity of PFe^{III}(C(O)R) with dioxygen has been monitored by ¹H and ²H NMR spectroscopy. Figure 7 shows the ¹H NMR spectra of (TAP)Fe^{III}(*n*-Bu) (trace A), (TAP)Fe^{III}(C(O)(*n*-Bu)) (trace B), and (TAP)Fe^{III}(C(O)(*i*-Bu)) (trace C). The results for the *n*-Bu complex parallel those reported earlier by Goff and co-workers.¹⁴ The patterns of resonances for the acyl complexes are characteristic of low-spin Fe^{III} porphyrins with the pyrrole protons shifted upfield. In comparison to the alkyl complexes, the acyl species shows pyrrole resonances which have larger line widths and smaller upfield shifts at any given temperature. Axial ligand resonances for the acyl groups are readily apparent in traces B and C of Figure 7. Comparison of intensities confirms the original assignment of the upfield shifted resonances at ca 2

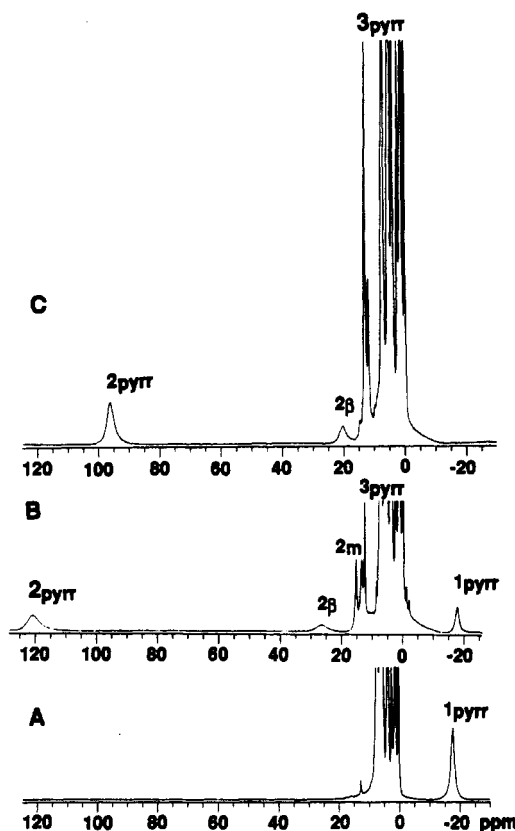


Figure 8. 300-MHz ^1H NMR spectra for the oxygenation of $(\text{TAP})\text{Fe}^{\text{III}}(\text{C}(\text{O})\text{Et})$ in dichloromethane solution: A, $(\text{TAP})\text{Fe}^{\text{III}}(\text{C}(\text{O})\text{Et})$ at $-70\text{ }^\circ\text{C}$; B, the same solution after adding dioxygen; C, the same solution after warming to $-30\text{ }^\circ\text{C}$. Resonances are assigned to individual species: 1, $(\text{TAP})\text{Fe}^{\text{III}}(\text{C}(\text{O})\text{Et})$; 2, $(\text{TAP})\text{Fe}^{\text{III}}(\text{OC}(\text{O})\text{Et})$; 3, $(\text{TAP})\text{Fe}^{\text{III}}\text{O}-\text{Fe}^{\text{III}}(\text{TAP})$. Subscripts give proton assignments following the scheme given in Figure 6, with m being the *meta*-anisyl protons.

ppm to the γ resonances of the substituent and the broad downfield shifted resonance to the β protons. The α protons are not observed, apparently because they are too broad to be detected.¹⁴ For $(\text{TAP})\text{Fe}^{\text{III}}(\text{C}(\text{O})(n\text{-Bu}))$ the δ methyl resonance is seen at 9 ppm but is not readily apparent in the figure.

The effect of addition of dioxygen to a sample of $(\text{TAP})\text{Fe}^{\text{III}}(\text{C}(\text{O})\text{Et})$ in dichloromethane is shown in Figure 8. Trace A shows the spectrum of $(\text{TAP})\text{Fe}^{\text{III}}(\text{C}(\text{O})\text{Et})$ alone at $-70\text{ }^\circ\text{C}$, while trace B shows the spectrum after admitting dioxygen to the sample. In trace B the pyrrole resonance of the acyl complex has diminished in intensity while resonances of two other species 2 and 3 have appeared. Trace C shows the effect of warming the sample to $-30\text{ }^\circ\text{C}$. At that point all of the acyl complex has been consumed. Resonances for 2 have shifted upfield, while that of 3 has shifted downfield. Further warming of the sample and recooling to either -30 or $-70\text{ }^\circ\text{C}$ reveals that 2 and 3 are stable entities which represent products of the reaction. Compound 2 shows the characteristic resonance pattern of a high-spin ($S = 5/2$), five-coordinate Fe^{III} porphyrin. Comparison with an authentic sample³⁴ shows that 2 is the carboxyl complex $(\text{TAP})\text{Fe}^{\text{III}}(\text{OC}(\text{O})\text{Et})$. The β methyl resonance of the axial ligand is apparent in the spectra. The α -methylene resonance is too broad to appear in the spectra at -70 and $-30\text{ }^\circ\text{C}$, but it is apparent at 30 ppm when the sample is warmed to $25\text{ }^\circ\text{C}$. The resonance labeled 3 in Figure 8 is readily identified as belonging to the antiferromagnetically coupled $(\text{TAP})\text{Fe}^{\text{III}}\text{O}-\text{Fe}^{\text{III}}(\text{TAP})$ on the basis of its chemical shift and the downfield shift that occurs upon warming.³⁵ The occurrence of $\text{PFe}^{\text{III}}\text{O}-\text{Fe}^{\text{III}}\text{P}$ as a product

(34) Arafa, I. M.; Goff, H. M.; David, S. S.; Murch, B. P.; Que, L., Jr. *Inorg. Chem.* **1987**, *26*, 2779.

(35) La Mar, G. N.; Eaton, G. R.; Holm, R. H.; Walker, F. A. *J. Am. Chem. Soc.* **1973**, *95*, 63.

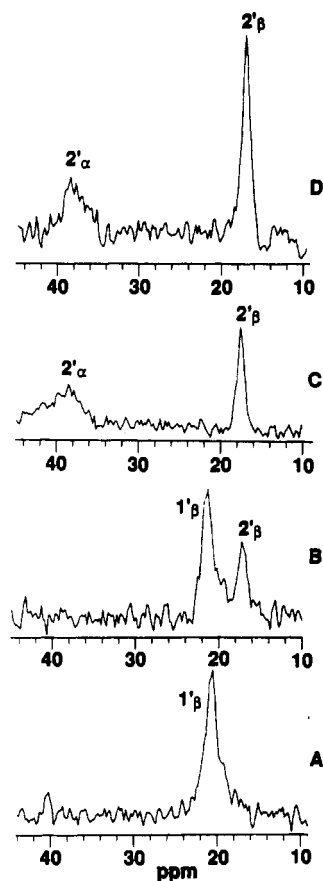


Figure 9. ^2H NMR spectra for the oxygenation of $(\text{TMP})\text{Fe}^{\text{III}}(\text{C}(\text{O})\text{C}_2\text{D}_5)$: A, $(\text{TMP})\text{Fe}^{\text{III}}(\text{C}(\text{O})\text{C}_2\text{D}_5)$ at $-70\text{ }^\circ\text{C}$; B and C, the sample 5 and 50 min after the addition of dioxygen at $-70\text{ }^\circ\text{C}$; D, the sample after warming to $25\text{ }^\circ\text{C}$ and recooling to $-70\text{ }^\circ\text{C}$. Resonance assignments follow the labeling in Figures 7 and 8. 1' is $(\text{TMP})\text{Fe}^{\text{III}}(\text{C}(\text{O})\text{C}_2\text{H}_5)$; 2' is $(\text{TMP})\text{Fe}^{\text{III}}(\text{OC}(\text{O})\text{C}_2\text{D}_5)$.

of oxygenation of $\text{PFe}^{\text{III}}(\text{C}(\text{O})\text{R})$ has been previously reported,¹⁴ but that study did not identify the carboxylate complex, $\text{PFe}^{\text{III}}(\text{OC}(\text{O})\text{R})$, as another product. The oxo-bridged dimer, $\text{PFe}^{\text{III}}\text{O}-\text{Fe}^{\text{III}}\text{P}$, may form as a result of hydrolysis of the carboxylate complex by adventitious water.

In order to explore the possible occurrence of ferryl intermediates in this oxygenation process, the reactivity of $(\text{TMP})\text{Fe}^{\text{III}}(\text{C}(\text{O})\text{Et})$ toward dioxygen has also been examined. With tetramesityl porphyrin two reactive ferryl complexes, red $(\text{TMP})\text{Fe}^{\text{IV}}=\text{O}$ ³⁶ and green $[(\text{TMP}^*)\text{Fe}^{\text{IV}}=\text{O}]^+$,^{22,23} are readily identified by their characteristic ^1H NMR spectra. Addition of dioxygen to $(\text{TMP})\text{Fe}^{\text{III}}(\text{C}(\text{O})\text{Et})$ in dichloromethane at $-80\text{ }^\circ\text{C}$ followed by warming reveals the formation of two high-spin complexes, $(\text{TMP})\text{Fe}^{\text{III}}(\text{OC}(\text{O})\text{Et})$ and $(\text{TMP})\text{Fe}^{\text{III}}\text{OH}$,³⁷ with pyrrole resonances at 114 and 116 ppm at $-70\text{ }^\circ\text{C}$. (In this case the hydroxy complex, rather than a μ -oxo dimer, is formed because the steric bulk of the four mesityl groups precludes the close approach of the two porphyrins that is necessary to form an oxo bridge.³⁷) Similarly addition of dioxygen to a solution of $(\text{TMP})\text{Fe}^{\text{III}}(\text{C}(\text{O})\text{Et})$ in toluene/methanol (4/1 v/v) yields ^1H NMR spectra which show the formation of $(\text{TMP})\text{Fe}^{\text{III}}\text{OH}$.³⁷ In both solvent systems, no evidence for the formation of the known compounds, $(\text{TMP})\text{Fe}^{\text{IV}}=\text{O}$ or $[(\text{TMP}^*)\text{Fe}^{\text{IV}}=\text{O}]^+$, was found during the oxygenation process.

In order to follow the behavior of the axial ligand during oxygenation, specifically deuterated $(\text{TMP})\text{Fe}^{\text{III}}(\text{C}(\text{O})\text{C}_2\text{D}_5)$ was prepared by carbonylation of $(\text{TMP})\text{Fe}^{\text{III}}(\text{C}_2\text{D}_5)$. Figure 9 shows

(36) Balch, A. L.; Chan, Y.-W.; Cheng, R.-J.; La Mar, G. N.; Latos-Grażyński, L.; Renner, M. W. *J. Am. Chem. Soc.* **1984**, *106*, 7779.

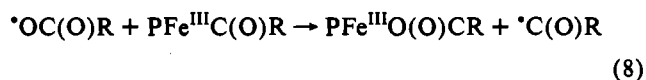
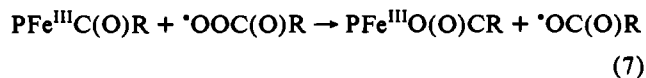
(37) Cheng, R. J.; Latos-Grażyński, L.; Balch, A. L. *Inorg. Chem.* **1982**, *21*, 2412.

^2H NMR spectra that were obtained during oxygenation of $(\text{TMP})\text{Fe}^{\text{III}}(\text{C}(\text{O})\text{C}_2\text{D}_5)$. Trace A shows the spectrum of the starting complex, $(\text{TMP})\text{Fe}^{\text{III}}(\text{C}(\text{O})\text{C}_2\text{D}_5)$ at -70°C . The resonance of the β -methyl group occurs at 21 ppm. Upon treatment with dioxygen, the spectra shown in traces B and C were obtained. Two new resonances at 38.5 and 19.5 ppm grow into the spectrum as the resonance from the starting material decreases in intensity. The product is thermally stable. Warming the sample to room temperature and recooling to -70°C produces the spectrum shown in trace D. The product responsible for these resonances is $(\text{TMP})\text{Fe}^{\text{III}}\text{OC}(\text{O})\text{C}_2\text{D}_5$.

Discussion

This work has resulted in isolation and structural characterization of low-spin iron(III) porphyrins with axial alkyl and acyl ligands. Both are structurally similar to $(\text{TPP})\text{Fe}^{\text{III}}\text{Ph}$. They have short Fe–N bonds, porphyrins with ruffled cores, and Fe–C distances in the range 1.955–1.979 Å. Both complexes are electron deficient, yet the methyl compound crystallizes as a THF solvate without coordination of the THF and the acyl compound has the simple monodentate structure. The presence of a monodentate acyl group in this electron-deficient environment contrasts with observations on the carbonylation of high-spin, 14-electron $(i\text{-Pr})_2\text{P}(\text{CH}_2)_2\text{P}(i\text{-Pr})_2\text{Fe}^{\text{II}}\text{Br}(\text{CH}_2\text{CMe}_3)$, which produces $(i\text{-Pr})_2\text{PCH}_2\text{CH}_2\text{P}(i\text{-Pr})_2\text{Fe}^{\text{II}}\text{Br}(\eta^2\text{-C}(\text{O})\text{CH}_2\text{CMe}_3)(\text{CO})$.²¹ In the latter, the bidentate coordination of the acyl group allows the product to achieve an 18-electron count. In that case the product is diamagnetic and hence low-spin. In the case of the porphyrin acyl, the geometry of the macrocycle and the constraints of short Fe–N bonds prohibit bidentate coordination by the axial ligand. The presence of the monodentate acyl group is consistent with the earlier observation of $\nu(\text{C}=\text{O})$ at 1817 cm^{-1} in $(\text{TPP})\text{Fe}(\text{C}(\text{O})(n\text{-Bu}))$.¹⁴

The iron(III) complexes with axial acyl ligands are reactive toward dioxygen. However, no evidence for the formation of an acyl peroxy complex of the type $\text{PFe}^{\text{III}}\text{O}_2\text{C}(\text{O})\text{R}$ has been observed. Moreover neither $(\text{TMP})\text{Fe}^{\text{IV}}=\text{O}$ nor $[(\text{TMP})\text{Fe}^{\text{IV}}=\text{O}]^+$ could be detected as intermediates during the oxygenation of $(\text{TMP})\text{Fe}^{\text{III}}\text{C}(\text{O})\text{R}$. In this regard, oxygenation of $\text{PFe}^{\text{III}}\text{C}(\text{O})\text{R}$ resembles that of $\text{PFe}^{\text{III}}\text{Ph}$ ²⁰ in that only stable products, $\text{PFe}^{\text{III}}\text{OC}(\text{O})\text{R}$ and $\text{PFe}^{\text{III}}\text{OPh}$, are observed during the oxygenation process. Our inability to directly observe the formation of an acyl peroxy complex could be caused by the low stability of such a species. However, the additional inability to observe the formation of any ferryl-containing complexes during these oxygenations suggests that acyl peroxy complexes may never form in the course of these reactions. To date the mechanism of dioxygen "insertion" into Fe–C bonds has received little direct study. For alkyl and acyl axial ligands it is possible that these insertions occur via a radical chain process which would be similar to that observed for organochromium(III) complexes.³⁸ For the acyl complexes this would require the presence of acyl radicals that could originate in the homolysis an Fe–C bond. A plausible route to the formation of the carboxylate product, without the formation of an acyl peroxy complex, is given in eqs 6–8. There



is ample evidence for the first step, the reaction of acyl radicals

Table 5. Crystal Structure Data

| | $(\text{TAP})\text{Fe}^{\text{III}}(\text{CH}_3)\cdot\text{THF}$ | $(\text{TAP})\text{Fe}^{\text{III}}(\text{C}(\text{O})(n\text{-Bu}))$ |
|--|--|---|
| formula | $\text{C}_{33}\text{H}_{39}\text{FeN}_4\text{O}_5$ | $\text{C}_{53}\text{H}_{43}\text{FeN}_4\text{O}_5$ |
| fw | 867.7 | 873.8 |
| space group | triclinic, $\bar{P}1$ | monoclinic, $P2_1/c$ |
| <i>a</i> , Å | 12.129(2) | 16.548(15) |
| <i>b</i> , Å | 12.263(3) | 18.699(9) |
| <i>c</i> , Å | 15.263(2) | 15.774(10) |
| α , deg | 71.93(2) | 90 |
| β , deg | 83.91(2) | 118.41(4) |
| γ , deg | 73.92(2) | 90 |
| <i>V</i> , Å ³ | 2073.3(7) | 4293(4) |
| <i>Z</i> | 2 | 4 |
| <i>T</i> , K | 130 | 130 |
| $\lambda(\text{Mo K}\alpha)$, Å | 0.710 69 | 0.710 69 |
| μ , mm ⁻¹ | 0.416 | 0.407 |
| <i>d</i> _{calc} , Mg/m ³ | 1.390 | 1.352 |
| transm factors | 0.97–0.98 | 0.87–0.94 |
| no. of reflns | 4858 | 1774 |
| no. of params | 586 | 258 |
| <i>R</i> ^a | 0.069 | 0.060 |
| <i>R</i> _w ^b | 0.076 | 0.050 |

$$^a R = \sum |F_o| - |F_c| / \sum |F_o|. \quad ^b R_w = \sum |F_o - |F_c||w^{1/2} / \sum |F_o|w^{1/2}.$$

with dioxygen to form acyl peroxy radicals.³⁹ The essential feature of this scheme that avoids the formation of an acyl peroxy complex is the attack of the acyl peroxy radical on an acyl ligand as shown in eq 7. The final reaction in the chain is the displacement to an acyl radical by a carboxyl radical, eq 8. Notice also that this scheme avoids the formation of any highly oxidized (e.g. ferryl) iron complex.

Experimental Section

Preparation of Compounds. Samples of $(\text{TAP})\text{Fe}^{\text{III}}\text{R}$ ($\text{R} = \text{CH}_3, \text{C}_2\text{H}_5, n\text{-Bu}$) and $(\text{TMP})\text{Fe}^{\text{III}}(\text{C}_2\text{H}_5)$ were prepared as described previously.^{3,8}

$(\text{TAP})\text{Fe}^{\text{III}}(\text{C}(\text{O})(n\text{-Bu}))$. Under a dinitrogen atmosphere, 0.082 mL (16.4 mmol) of a 2 M solution of $n\text{-BuMgCl}$ in diethyl ether was added to a green-brown solution of 125 mg (15 mmol) of $(\text{TAP})\text{Fe}^{\text{III}}\text{Cl}$ in 50 mL of toluene. The mixture, which assumed a red color due to the formation of $(\text{TAP})\text{Fe}^{\text{III}}(n\text{-Bu})$, was stirred for 1 min. A stream of carbon monoxide was bubbled through the red solution for 10 min. The red solution was cooled to -40°C and allowed to stand at that temperature for 1 h. The solvent was removed by vacuum evaporation, and the solid product was dried under vacuum for 12 h. The solid was dissolved in a minimum volume of dichloromethane, and the solution was subjected to chromatography on a 5×2.2 cm column of activated alumina with dichloromethane as the eluent. The first red band which eluted rapidly was collected and evaporated to dryness to give the product (21 mg, 16% yield). Other acyl complexes were prepared similarly.

X-ray Data Collection. Red prisms of $(\text{TAP})\text{Fe}^{\text{III}}(\text{CH}_3)\cdot\text{THF}$ were grown by diffusion of hexane into a solution of the complex in a mixture of toluene and THF. A suitable crystal was coated with a light hydrocarbon oil and mounted in the 130 K dinitrogen stream of a Siemens P4/RA diffractometer that was equipped with a locally modified LT-2 low-temperature apparatus. Brown plates of $(\text{TAP})\text{Fe}^{\text{III}}(\text{C}(\text{O})(n\text{-Bu}))$ were grown by diffusion of hexane into a toluene solution of the complex. A suitable crystal was treated as described above and placed in the 130 K dinitrogen stream of a Siemens R3m/v diffractometer that was equipped with an Enraf-Nonius low-temperature device. Two check reflections showed random (<2%) variation during each data collection. The data were corrected for Lorentz and polarization effects. Crystal data are given in Table 5.

Solution and Refinement of Structures. $(\text{TAP})\text{Fe}^{\text{III}}(\text{CH}_3)\cdot\text{THF}$. Calculations were performed with the Siemens SHELXTL PLUS version 4.0 software package. The structure was solved by Patterson methods. Anisotropic thermal parameters were assigned to the iron, oxygen, nitrogen, and carbon atoms. Hydrogen atoms were refined at calculated positions through the use of a riding model in which the C–H vector was fixed at 0.96 Å. Scattering factors and corrections for anomalous

(38) Ryan, D. A.; Espenson, J. H. *J. Am. Chem. Soc.* **1982**, *104*, 704.

(39) Walling, C. *Free Radicals in Solution*; John Wiley and Sons: New York, 1957; p 401.

dispersion were taken from a standard source.⁴⁰ There was disorder at the THF site, and two positions were found for the oxygen atom and one of the adjacent carbon atoms. The final stages of refinement included an absorption correction with a method that obtains an empirical absorption tensor from an expression that relates F_o and F_c .⁴¹ The largest peak in the final difference map had a value of $0.56 \text{ e } \text{\AA}^{-3}$.

(TAP)Fe^{III}(C(O)(*n*-Bu)). Calculations were performed with the Siemens SHELXTL PLUS version 4.2 software package. The structure was solved by direct methods. Anisotropic thermal parameters were assigned to the iron atom only. Hydrogen atoms were refined at calculated positions through the use of a riding model in which the C-H vector was

fixed at 0.96 Å. An absorption correction was applied. The largest peak in the final difference map had a value of $0.35 \text{ e } \text{\AA}^{-3}$.

Instrumentation. ¹H and ²H NMR spectra were recorded on a General Electric QE 300 Fourier transform spectrometer.

Acknowledgment. We thank the NIH (Grant GM26226) for financial support and Professor W. R. Scheidt and Professor R. H. Beer for informative discussions.

Supplementary Material Available: Tables of bond distances, bond angles, anisotropic thermal parameters, hydrogen atom coordinates, and crystal structure refinement data for (TAP)Fe^{III}(CH₃)·THF and (TAP)-Fe^{III}(C(O)(*n*-Bu)) (15 pages). Ordering information is given on any current masthead page.

(40) *International Tables for X-ray Crystallography*; D. Reidel Publishing Co.: Boston, MA, 1992; Vol. C.

(41) Moezzi, B. Ph.D. Thesis, University of California, Davis, CA, 1987.